

# All-optical switching of a single resonance in silicon ring resonators

Y. Henry Wen,<sup>1</sup> Onur Kuzucu,<sup>1</sup> Taige Hou,<sup>2</sup> Michal Lipson,<sup>2,3</sup> and Alexander L. Gaeta<sup>1,\*</sup>

<sup>1</sup>*School of Applied and Engineering Physics, Cornell University, Ithaca, New York 14853, USA*

<sup>2</sup>*School of Electrical and Computer Engineering, Cornell University, Ithaca, New York 14853, USA*

<sup>3</sup>*Kavli Institute at Cornell for Nanoscale Science, Cornell University, Ithaca, New York 14853, USA*

\*Corresponding author: a.gaeta@cornell.edu

Received February 17, 2011; accepted March 2, 2011;  
 posted March 21, 2011 (Doc. ID 142844); published April 13, 2011

We theoretically investigate a wavelength-selective all-optical switch using Raman-induced loss in a silicon resonator add-drop filter. We show that picojoule control pulses can selectively modulate and “erase” a single cavity resonance from full extinction to greater than 97% transmission while leaving adjacent resonances undisturbed. Full switching is achievable in less than 300 ps with only a few hundred femtojoule energy dissipation. This represents, to our knowledge, the first scheme for selective modulation of single resonances of an optical cavity. © 2011 Optical Society of America

OCIS codes: 130.4815, 130.3990, 290.5910.

Integrated silicon photonics is the natural choice for chip-based, high-speed optical signal processing due to its compatibility with complementary metal-oxide-semiconductor (CMOS) technology and transparency to standard telecommunications wavelengths [1]. Central to its success are low-loss optical switching and routing [2]. Efficient all-optical switching in silicon has been demonstrated primarily in resonant devices using the Kerr nonlinearity or free-carrier refraction [3–6]. These nonlinear refractive effects are broadband and simultaneously affect all resonances of a cavity [6]. While this is desirable in many applications, the full functionality of an all-optical router is realized only if separate channels can be modulated independently.

In resonant structures it is also possible to achieve all-optical switching by changing the coupling condition through optically induced loss. Increasing the loss of a critically coupled resonator will significantly increase transmission on-resonance, and this has been termed “Zeno switching” [7]. It is therefore possible to achieve wavelength-selective switching and routing using a narrowband absorption feature in a multiport resonator.

Raman-induced loss in silicon is ideal for wavelength-selective all-optical switching. Inverse Raman scattering in silicon produces strong loss at the anti-Stokes wavelength [8], with a bandwidth much narrower than the free spectral range of a typical microring cavity but wider than the resonance linewidth. It is tunable simply by changing the control wavelength. This allows the Raman loss to modulate a single resonance while leaving adjacent resonances undisturbed. Loss-based switches have also been proposed using two-photon absorption (TPA) in atomic vapor [7] or difference frequency generation in III–V materials [9] as the loss mechanism. However, both systems require more complicated fabrication and/or operation.

In this Letter we propose a wavelength-selective all-optical switch based on Raman-induced loss in a silicon microring add-drop filter. We show that gigahertz-rate picojoule control pulses are able to modulate a single resonance at the anti-Stokes wavelength from full extinc-

tion to >97% transmission with energy loss of only hundreds of femtojoules per bit.

Consider a weak anti-Stokes signal (blue) and a strong control (red), both resonant with the ring and coupled into their respective in-ports (Fig. 1). For both the control and the signal to be simultaneously resonant, the ring’s free spectral range (FSR) must be equal to an integer fraction of the Raman shift  $\Omega_R$ . The coupling region can be modeled as an asymmetric beam splitter with field amplitude transmissivity  $t_1$  and reflectivity  $r_1 = i\sqrt{1 - t_1^2}$ . Similarly, the coupling to the drop waveguide is characterized by  $t_2$  and  $r_2 = i\sqrt{1 - t_2^2}$ . Following the analysis in [7] we obtain the on-resonance [i.e.,  $\lambda_{\text{res}} = n(\lambda_{\text{res}})m$ , where  $m$  is the mode order] through-port transmission for the anti-Stokes signal,

$$T_N(\lambda_{\text{res}}) = \left[ \frac{t_1 - \alpha t_2}{1 - \alpha t_1 t_2} \right]^2, \quad (1)$$

where  $\alpha = e^{-a(\lambda)L/2}$ ,  $L$  is the circumference of the ring, and  $a(\lambda)$  and  $n(\lambda)$  are the loss coefficient and the refractive index, respectively.

In the absence of the control, the total loss is the intrinsic loss of the ring,  $a(\lambda) = a_1$ . Critical coupling is obtained for  $\alpha = |t_1|/|t_2|$  when the round trip loss is matched by the ratio of the bus waveguide and drop

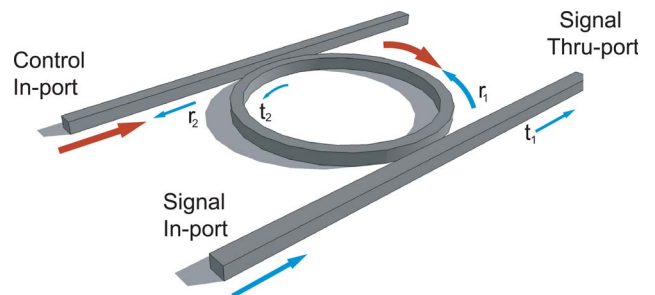


Fig. 1. (Color online) Add-drop filter with counterpropagating control (red) and anti-Stokes signal (blue). Transmission is observed as the signal through-port. The control in-port also serves as the signal drop-port.

waveguide coupling rates. The through-port transmission  $T_N(\lambda_{\text{res}}) = 0$ , and the drop-port transmission is unity. The through-port transmission spectrum of the add-drop filter with  $Q = 200,000$  is plotted in Fig. 2(a). Since the linewidth is extremely narrow, the resonances appear as single lines.

In the presence of the control, the ring becomes more lossy due to Raman-induced loss  $a_R(\lambda)I_c$ . The control also introduces a Kerr index shift and generates free carriers through TPA. The free carriers lead to free-carrier absorption (FCA) and free-carrier refraction (FCR). However, all the deleterious effects can be significantly reduced by using a p-i-n diode to shorten the carrier lifetime, as we will discuss later. The loss and refractive index have the following form, with the Raman loss being the dominant term:

$$\begin{aligned} a(\lambda) &= a_1 + a_{\text{fca}} + a_R(\lambda)I_c, \\ n(\lambda) &= n_0(\lambda) + n_{\text{fcr}} + n_2I_c. \end{aligned} \quad (2)$$

As the Raman-induced loss increases (smaller  $\alpha$ ), the transmission increases from full extinction to the maximum value of  $t_1^2$ . For low intrinsic loss,  $t_1^2$  is nearly unity and  $T_N$  is a sensitive function of  $I_c$ . Thus the transmission on-resonance can be modulated for a critically coupled resonator between total extinction and full transmission (Fig. 3 inset), with no change to the transmission of the other resonances.

The magnitude of the induced Raman loss depends linearly on the intensity of the control field inside the ring, and the loss is blueshifted from the control by the Raman frequency  $\Omega_R$  of the material with a bandwidth of  $\Gamma_R$ . For silicon the Raman frequency  $\Omega_R = 15.6$  THz and band-

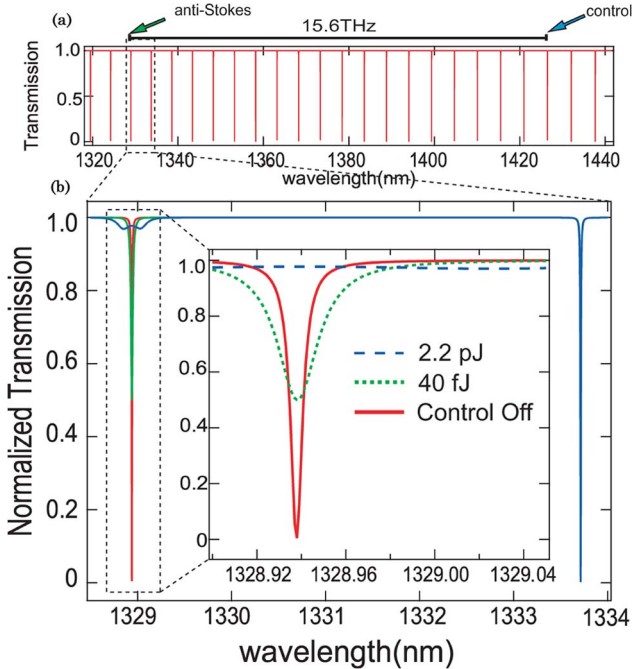


Fig. 2. (Color online) (a) Passive transmission spectrum of high- $Q$  silicon add-drop filter. The control and anti-Stokes signal are tuned to resonances 15.6 THz apart. (b) Transmission at the anti-Stokes resonance for several control pulse energies. Adjacent resonances are undisturbed.

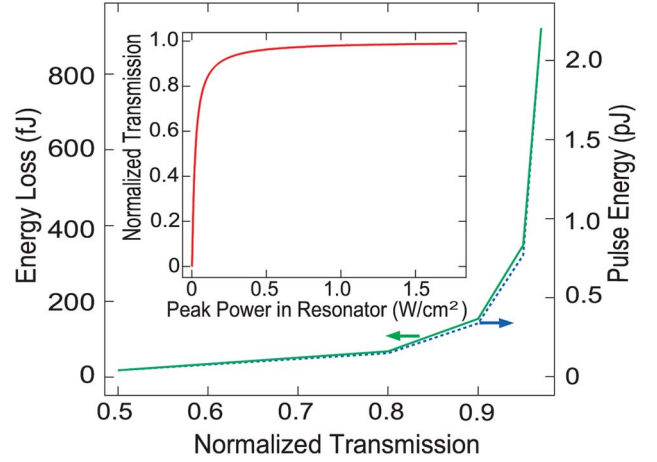


Fig. 3. (Color online) Control pulse energy and energy dissipation required to achieve certain transmission. Inset: Transmission as a function of power inside the cavity. Switching is most efficient for transmission values below 90%.

width  $\Gamma_R = 105$  GHz [8]. The strength of the Raman loss in silicon is found by normalizing the peak of the Raman gain at the Stokes wavelength to the experimentally obtained values for peak Raman gain  $g_R = 76$  cm/GW for  $\lambda_c = 1430$  nm [10]. The highest Raman gains were observed for shorter control wavelengths and control pulses longer than the Raman ringdown time of 10 ps [11]. Here we consider control pulses in the range of 200–300 ps at 1430 nm and the anti-Stokes signal near 1330 nm. Close to the anti-Stokes frequency  $\omega_a = \omega_c + \Omega_R$ , Raman loss in silicon is

$$a_R(\omega) = \frac{g_R \Gamma_R^2}{(\omega - \omega_a)^2 + \Gamma_R^2}. \quad (3)$$

We assume a waveguide dimension of  $250 \text{ nm} \times 450 \text{ nm}$  and a ring diameter of  $32 \mu\text{m}$  ( $L = 100 \mu\text{m}$ ), which corresponds to an FSR equal to an integer fraction of the Raman shift, so the control and anti-Stokes wavelengths are simultaneously resonant. We assume linear loss of 1.74 dB/cm, which corresponds to an intrinsic  $Q = 400,000$ . These values have been demonstrated with current fabrication techniques [12]. An output coupling of  $t_2 = 0.9998$  is chosen, corresponding to  $t_1 = 0.996$ , resulting in  $Q = 200,000$ . This provides field enhancement to both the control and anti-Stokes beams in the ring by a nominal factor of  $F/\pi$ , where  $F = \text{FSR}/(\nu)$  is the finesse of the cavity. The free-carrier density can be calculated according to the rate equation  $\partial N_e/\partial t = \beta_{\text{TPA}} I_c^2 / 2\hbar\omega_0 - N_e/\tau_c$  [13], where  $\beta_{\text{TPA}} = 0.5 \text{ cm/GW}$ . We assume a p-i-n diode swept free-carrier lifetime of  $\tau_c = 12$  ps [14], in which case FCA becomes negligible compared to the Raman-induced loss. FCR is still sufficient to blueshift the resonance by more than a linewidth, but this effect becomes comparable to the redshift from the Kerr nonlinearity. For the control intensities under consideration, these two effects effectively cancel out.

The transmission at the anti-Stokes wavelength is plotted for 1427.7 nm control pulses at several energies [Fig. 2(b)]. On-resonance transmission of 50% (90%) is achievable with a control pulse of 40 fJ (340 fJ)/bit with energy dissipation of 18 fJ (154 fJ)/bit. Transmission of

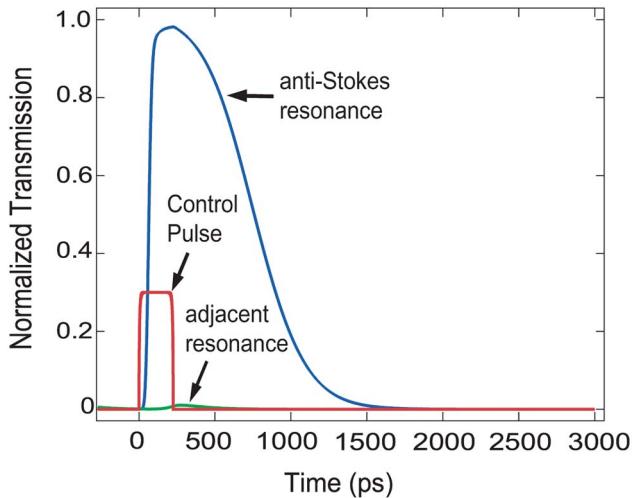


Fig. 4. (Color online) Response of anti-Stokes signal at through-port to 2.2 pJ, 300 ps control pulse. Ninety-seven percent transmission is achieved with the adjacent resonance essentially undisturbed.

>97% (<0.1 dB loss) is achievable with control pulses of 2.2 pJ/bit and energy dissipation of 921 fJ/bit (Fig. 3). These values are comparable with carrier and Kerr-based switches in silicon microrings [3,5]. It is noteworthy that the narrowband Raman response leaves adjacent resonances essentially undisturbed, which opens up the possibility of independent routing or modulation of multiple signals on a single resonator.

Switching is most efficient for transmission below 90% but rolls off for higher transmission (Fig. 3). The roll-off value increases for lower intrinsic loss, so higher- $Q$  resonators yield better switching performance. At higher control energies, cavity enhancement decreases due to FCA and TPA. The enhancement  $F/\pi$  has a nominal value of 250 but decreases with increasing control pulse energy and is 4 times lower for the 2.2 pJ pulse than for the 40 fJ pulse. Thus, operating below 90% transmission will significantly reduce power consumption.

Time-domain switching dynamics confirm the independent switching of a single resonance at gigahertz rates (Fig. 4). A 2.2 pJ control pulse achieves maximum transmission of 97%, matching the results of the frequency-domain analysis (Fig. 2). The adjacent resonance sees a 1% increase in transmission due to broadband FCA. The switch-on time, defined as the time required for the signal to be fully switched from the drop-port to

the through-port, is less than 300 ps, and the total response time for a full switching cycle is roughly 1.5 ns. This corresponds to data rates of >500 MHz on a single channel with rates of >1 GHz possible at lower switching contrasts.

The Raman-loss all-optical switch enables independent switching and routing of multiple channels in integrated silicon photonic networks. This device is compatible with CMOS processing and relies entirely on the intrinsic properties of the waveguide material. The ability to switch a single channel, combined with conventional switching mechanisms, gives flexibility to both hardware and software design for on-chip optical systems.

The authors would like to acknowledge the Defense Advanced Research Projects Agency (DARPA) for supporting this work under the Zeno-based OptoElectronics program.

## References

1. M. Paniccia and R. Won, *Nat. Photon.* **4**, 498 (2010).
2. G. T. Reed, G. Mashanovich, F. Y. Gardes, and D. J. Thomson, *Nat. Photon.* **4**, 518 (2010).
3. A. Martínez, J. Blasco, P. Sanchis, J. V. Galán, J. García-Rupérez, E. Jordana, P. Gautier, Y. Lebour, S. Hernández, R. Spano, R. Guider, N. Daldosso, B. Garrido, J. M. Fedeli, L. Pavesi, and J. Martí, *Nano Lett.* **10**, 1506 (2010).
4. M. Belotti, M. Galli, D. Gerace, L. C. Andreani, G. Guizzetti, A. R. Md Zain, N. P. Johnson, M. Sorel, and R. M. De La Rue, *Opt. Express* **18**, 1450 (2010).
5. V. R. Almeida, C. A. Barrios, R. R. Panepucci, and M. Lipson, *Nature* **431**, 1081 (2004).
6. B. G. Lee, A. Biberman, P. Dong, M. Lipson, and K. Bergman, *IEEE Photon. Technol. Lett.* **20**, 767 (2008).
7. B. C. Jacobs and J. D. Franson, *Phys. Rev. A* **79**, 063830 (2009).
8. D. R. Solli, P. Koonath, and B. Jalali, *Phys. Rev. A* **79**, 053853 (2009).
9. Y.-P. Huang and P. Kumar, *Opt. Lett.* **35**, 2376 (2010).
10. Z. R. Claps, D. Dimitropoulos, V. Raghunathan, Y. Han, and B. Jalali, *Opt. Express* **11**, 1731 (2003).
11. H. K. Tsang and Y. Liu, *Semicond. Sci. Technol.* **23**, 064007 (2008).
12. S. Xiao, M. H. Khan, H. Shen, and M. Qi, *Opt. Express* **15**, 14467 (2007).
13. R. Soref and B. Bennett, *IEEE J. Quantum Electron.* **23**, 123 (1987).
14. A. C. Turner-Foster, M. A. Foster, J. S. Levy, C. B. Poitras, R. Salem, A. L. Gaeta, and M. Lipson, *Opt. Express* **18**, 3582 (2010).